JOURNAL OF VIROLOGY, July 2005, p. 8894–8903 Vol. 79, No. 14
0022-538X/05/$08.00+0 doi:10.1128/JVI.79.14.8894–8903.2005

Pathogenesis of Human Metapneumovirus Lung Infection in BALB/c Mice and Cotton Rats

Marie-Ève Hamelin,[1]* Kevin Yim,[2] Katie H. Kuhn,[2] Rose P. Cragin,[2] Marina Boukhvalova,[2] Jorge C. G. Blanco,[2] Gregory A. Prince,[2] and Guy Boivin[1]*

Research Center in Infectious Diseases of the Centre Hospitalier Universitaire de Québec, and Laval University, Québec City, Québec, Canada,[1] and Virion Systems, Inc., Rockville, Maryland[2]

Received 26 November 2004/Accepted 22 March 2005

Human metapneumovirus (hMPV) is a newly described member of the *Paramyxoviridae* family causing acute respiratory tract infections, especially in young children. We studied the pathogenesis of this viral infection in two experimental small animal models (BALB/c mice and cotton rats). Significant viral replication in the lungs of both animals was found following an intranasal challenge of 10^8 50% tissue culture infectious doses ($TCID_{50}$) and persisted for <2 and <3 weeks in the case of cotton rats and mice, respectively. Peak viral loads were found on day 5 postinfection in both mice (mean of 1.92×10^7 $TCID_{50}$/g lung) and cotton rats (mean of 1.03×10^5 $TCID_{50}$/g). Clinical symptoms consisting of breathing difficulties, ruffled fur, and weight loss were noted in mice only around the time of peak viral replication. Most significant pulmonary inflammatory changes and peak expression of macrophage inflammatory protein 1α, gamma interferon, and RANTES occurred at the time of maximal viral replication (day 5) in both models. Cellular infiltration occurred predominantly around and within alveoli and persisted for at least 21 days in mice, whereas it was more limited in time with more peribronchiolitis in cotton rats. Both animal models would be of great value in evaluating different therapeutic agents, as well as vaccine candidates against hMPV.

The human metapneumovirus (hMPV) is a newly described viral pathogen (*Paramyxoviridae* family, *Pneumovirinae* subfamily, and genus *Metapneumovirus*) first reported in young Dutch children with acute respiratory tract infections (ARTI) (42). Since its initial discovery in 2001, hMPV has been identified in many countries from all continents, indicating its worldwide distribution (20). Serological studies have shown that hMPV is a ubiquitous virus that virtually infects all children by the age of 5 to 10 years (14, 42, 49). In addition, studies from The Netherlands have indicated that the virus has been circulating in humans for at least 50 years (42). Several reports have associated hMPV with ARTI in all age groups with more severe diseases such as bronchiolitis/bronchitis and pneumonia occurring in young children, elderly individuals, and immunocompromised hosts (8, 9, 16, 20, 44, 48). By reverse transcription-PCR methods, hMPV has been found in 5 to 10% of children hospitalized for ARTI (8, 9, 15, 17), as well as in children with acute wheezing and asthma exacerbation (23, 31).

The hMPV genome consists of a single-stranded negative RNA molecule of approximately 13 kb containing eight genes encoding nine proteins. hMPV isolates can be separated into two major groups (A and B) and at least four subgroups, based mainly on genetic data and, to some extent, on antigenic properties (8, 10, 21, 32, 43). Overall nucleotide and amino acid sequence identities between two Canadian strains representing the two major hMPV groups were found to be 80 and 90%, respectively, with the highest variability occurring in the attachment (G) and SH genes (5). HMPV replicates slowly in a few permissive cell lines, including tertiary monkey kidney and Vero cells (8, 32, 42), which is probably the reason for its late identification.

A few experimental animal models of hMPV infection have been reported so far. Viral replication has been found in the respiratory tract of experimentally infected chimpanzees and monkeys (cynomolgus monkeys, rhesus macaques, and African green monkeys) and was associated with mild upper respiratory tract signs in some of these animals (26, 28, 42). Some groups have also shown that hMPV can replicate in the lungs of hamsters without the appearance of recognizable clinical signs (28, 37, 40). Recently, Alvarez et al. have reported efficient hMPV replication in lungs of BALB/c mice associated with transient weight loss (1). BALB/c mice and especially cotton rats are considered good and convenient experimental models to study the pathogenesis of human respiratory syncytial virus (hRSV), another paramyxovirus (7, 11, 12, 19, 22, 24, 45, 46, 50).

In this study, we sought to characterize the pathogenesis of hMPV lung infection in those two small animal models. Our results indicate that both animals efficiently support viral replication, which was associated in infected mice with significant lung inflammation, weight loss, and breathing difficulties. Such experimental models would be of great interest for the evaluation of different therapeutic agents and vaccine candidates.

MATERIALS AND METHODS

Cell line and virus. LLC-MK2 cells were maintained in minimal essential medium (Gibco/BRL, Bethesda, MD) supplemented with 10% fetal bovine serum. HMPV strain C-85473 (group A as CAN97-83 and NL/00-1) is a clinical strain passed six times on LLC-MK2. It was grown on LLC-MK2 cells in minimal essential medium supplemented with 0.2% glucose, 0.1% bovine serum albumin, 0.0002% trypsin, and 1% gentamicin (hMPV infection medium).

* Corresponding author. Mailing address: CHUQ-CHUL, Room RC-709, 2705 Blvd. Laurier, Sainte-Foy, Québec, Canada G1V 4G2. Phone: (418) 654-2705. Fax: (418) 654-2715. E-mail for Guy Boivin: Guy.Boivin@crchul.ulaval.ca. E-mail for Marie-Ève Hamelin: Marie-eve.Hamelin@crchul.ulaval.ca.

HMPV quantification. Virus titers were determined by 10-fold serial dilutions of virus in 24-well plates containing LLC-MK2 cells. Before infection, cells were washed twice with phosphate-buffered saline (PBS) to remove residual serum proteins that could inhibit trypsin activity. Infected plates were incubated at 37°C with 5% CO_2 and replenished with 1 μl of fresh trypsin (0.0002%) every other day. Virus titers were reported as $\log_{10}$ 50% tissue culture infectious doses ($TCID_{50}$) per milliliter of culture supernatant or per gram of lung. The lower limit of detection of our assay was 10^2 $TCID_{50}$ per gram. $TCID_{50}$ were calculated by the Reed and Muench method.

BALB/c and cotton rat studies. Experiments were performed in two different laboratories by initially infecting 108 4- to 6-week-old BALB/c mice (Charles River Laboratories, Wilmington, MA) and 36 young adult cotton rats (*Sigmodon hispidus*) (colony maintained at Virion Systems, Inc., Rockville, MD). The animals were infected intranasally with 10^8 $TCID_{50}$ of hMPV strain C-85473 in 25 μl (mice) or 100 μl (cotton rats) of hMPV infection medium. The same number of animals was sham infected with infection medium, and all animals were housed in groups of five in microisolator cages for the mice and in polycarbonate cages for the cotton rats. The animals were evaluated on a daily basis for mortality, weight loss, and presence of any respiratory symptoms. At serial times postinfection (days 1, 3, 5, 7, 12, and 21), lungs and blood samples were collected from 18 mice and six cotton rats from both hMPV- and sham-infected groups.

Virus titration in lungs. At the specified time points, the animals were sacrificed, and the lungs were removed and quickly frozen in liquid nitrogen. Both lungs were used for viral titration in the case of mice, whereas the upper right lobe was used for cotton rats. Whole lungs were also used for cotton rats on day 5 postinfection to compare virus titers with those obtained from the upper right lobe only. Lungs were weighed, homogenized in 1 ml of hMPV infection medium, and laid on LLC-MK2 monolayers for virus titration as reported above. Virus titers in lungs of both animals were determined at a single center.

Pulmonary histopathology. Lungs were removed and fixed with 10% buffered formalin. Fixed lungs were embedded in paraffin, sectioned in 5-μm slices, and stained with hematoxylin-eosin. Both lungs were used for mice whereas the left lung was used in the case of cotton rats at all time points. In addition, whole lungs were also used for cotton rats on day 5 postinfection to compare the inflammatory changes with those described in the left lung only. The histopathologic score (HPS) for both animals was determined by two independent researchers at a single institution who were unaware of the infection status of the animals. Four types of histopathological changes were scored independently in each lung section: peribronchiolitis (inflammatory cells, primarily lymphocytes, surrounding a bronchiole), perivasculitis (inflammatory cells, primarily lymphocytes, surrounding a blood vessel), interstitial pneumonitis (increased thickness of alveolar walls associated with inflammatory cells, primarily neutrophils), and alveolitis (inflammatory cells, primarily neutrophils and macrophages, within alveolar spaces). Each histopathological change was scored on a scale of 0 (no change) to 4 (maximum inflammation), with a score of 4 being based upon our prior observations of maximal pathological changes induced by hRSV infection of cotton rat lungs (35).

Type of inflammatory cells. Cell recruitment in bronchoalveolar lavage (BAL) samples was determined with mice and cotton rats. In brief, six animals were sacrificed at different times (1, 3, 5, or 7 days postinfection), and then their tracheae were cannulated with a catheter. Several 1.0-ml injections of PBS were done until a total of 3 ml of BAL fluid was collected. For hMPV-infected mice, BAL was centrifuged at 1,800 × *g* for 10 min at 4°C, and then cell pellets were resuspended in PBS for leukocyte quantification using a hemacytometer. Specific cell populations were distinguished using hematoxylin- and eosin-stained cytospin preparations. The relative cell counts were calculated from a total of 2.5×10^5 cells. For hMPV-infected cotton rats, specific cell populations were distinguished by FACSCalibur (Becton-Dickinson, Franklin Lakes, NJ), and 10^4 cells were sorted to calculate the percentage of cell types.

Pulmonary cytokine levels. To determine cytokine levels, both lungs were used for mice, whereas the lower lobe of the right lung was used for cotton rats. Lungs were homogenized in 1.5 ml of cold potassium buffer (50 mMKPO_4, pH 6.0), and 750 μl of the homogenate was mixed with 750 μl of potassium buffer containing 0.2% CHAPS {3-[(3-cholamidopropyl)-dimethylammonio]1-1-propanesulfonate} and 0.2% of a protease inhibitor cocktail (both from Sigma, St. Louis, MO). Samples were centrifuged at 13,800 × *g* for 10 min at 4°C, and 50 μl of the supernatant was used for cytokine quantification of samples from mice by ELISA. Levels of monocyte chemotactic protein 1 (MCP-1), macrophage inflammatory protein 1α (MIP-1α), RANTES, the mouse interleukin 8 (IL-8) homologue KC, and gamma interferon (IFN-γ) were determined using reagents (specific antibodies and recombinant cytokines) obtained from R&D Systems, Inc. (Minneapolis, MN). Conjugate streptavidin-horseradish peroxidase was purchased from RDI (Flanders, NJ). IL-4 levels were determined with the commercial Quantikine mouse kit (R&D Systems).

Quantification of MCP-1, MIP-1α, RANTES, IFN-γ, and IL-2 was performed with lungs of cotton rats by densitometric analysis of mRNA expression. Total RNA was isolated from cotton rat lung tissues with a commercial RNA isolation kit (Midi-RNeasy Kit; QIAGEN, Chatsworth, CA). One microgram of total RNA from lung tissues was utilized to prepare cDNA using oligo(dT) primers and the SuperScript II reverse transcriptase (Invitrogen, Burlington, Ontario). Fifty picograms of cDNA constructs was used for the PCR. The forward and reverse primers for the cotton rat cytokines and the PCR conditions have been previously described (6, 7). Amplified products of target cytokines were electrophoresed and transferred to nylon Hybond N^+ membranes (Amersham Pharmacia Biotech, Piscataway, NJ) in 10× SSC (1× SSC is 0.15 M NaCl plus 0.015 M sodium citrate) by a standard Southern blot procedure. DNA was UV cross linked and hybridized to an internal oligonucleotide probe (7). Labeling of the probe and subsequent detection of bound probe were carried out with an enhanced chemiluminescence (ECL) system (Amersham Pharmacia Biotech), followed by exposure to X-OMAT AR autoradiography film (Kodak, Rochester, NY). The resulting blots were scanned using Cannon N650U and analyzed using Scion Image software. In brief, a Southern blot scan in a grayscale mode was resized using Adobe Photoshop 6.0 to the image width of 400 pixels and saved in a TIFF format. The file was then opened in the Scion Image program and the Mean Density (average gray value within the selection) measurement option was selected. The boxes of identical size were placed around each band on the scan corresponding to amplified cDNA, and mean density within those boxes was recorded. Three additional boxes were placed randomly on the area of the scan away from the bands to obtain background readings. The average of these background readings were used to normalize the rest of the measurements against them. The signal obtained for each analyzed gene was then normalized to the level of β-actin expressed in the corresponding organ.

Statistical analysis. All data, with the exception of the histopathologic score, are expressed as mean ± standard deviation. For data that were normally distributed, Student's *t* test was used to compare hMPV-infected and sham-infected groups of animals at the same time point. Alternatively, the Mann-Whitney sum test was used for comparisons of data that were not normally distributed.

RESULTS

Clinical manifestations of hMPV infection in mice and cotton rats. Mice and cotton rats were infected with 10^8 $TCID_{50}$ of hMPV (strain C-85473) and were observed on a daily basis for mortality, weight loss, and presence of any respiratory symptoms. On day 1 postinfection, mice began to have ruffled hair that persisted until day 7. Breathing problems appeared on day 4 to 5 postinfection, as well as a slight decrease in physical activity and a tendency to huddle. Significant weight loss between hMPV-infected and sham-infected mice was noted on days 4 to 10 with maximal decrease on day 7 (mean weight loss of 18.2%) (Fig. 1). Gradual normalization of the weight and the other clinical parameters occurred after day 10. One of the 36 remaining hMPV-infected mice died between days 7 and 8 postinfection. No mortality, weight loss, or respiratory symptoms were observed in hMPV-infected cotton rats as well as in any of the sham-infected mice or cotton rats.

Virus titers in lungs. Mean hMPV $TCID_{50}$ per gram of mouse lungs were 2.14×10^4, 1.58×10^6, 1.92×10^7, 3.30×10^3, and 2.49×10^2 on days 1, 3, 5, 7, and 12 postinfection, respectively. Similarly, virus titers were 8.78×10^2, 8.1×10^3, 1.03×10^5, 3.72×10^2, and undetectable ($<10^2$ $TCID_{50}$/g) in lungs of cotton rats (Fig. 2). Of note, virus titers determined from whole lungs of hMPV-infected cotton rats were similar (1.39×10^5 $TCID_{50}$/g) to those found in the upper right lobe on day 5 postinfection. No viruses were recovered on day 21 in hMPV-infected animals or at any time points in sham-infected mice or cotton rats.

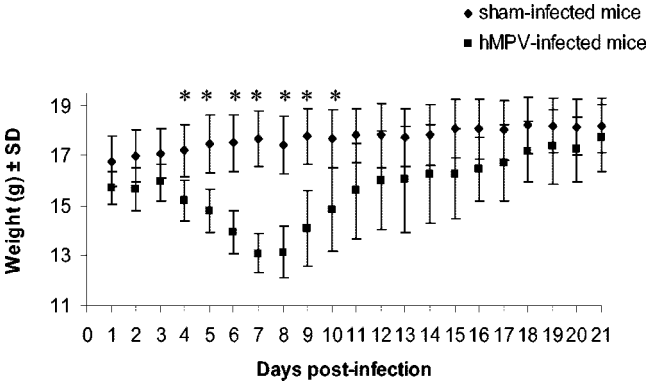

FIG. 1. Daily mean weights of hMPV- and sham-infected mice. Eighteen mice were sacrificed at serial times postinfection (days 1, 3, 5, 7, 12, and 21), beginning with 108 mice per group. *, statistically significant differences ($P < 0.05$) in weight were observed on days 4 to 10 postinfection, based on the Mann-Whitney rank sum test. SD, standard deviation.

Histopathologic changes in lungs. Pulmonary inflammation was assessed using a scoring scale system previously described in cotton rats with hRSV infection (35). Peak inflammatory response (i.e., the highest HPS) occurred at the time of maximal virus replication (day 5) in both animal models (Fig. 3). This consisted mostly of an interstitial inflammation (characterized by the increased thickness of alveolar walls) and the presence of alveolitis (characterized by the presence of inflammatory cells within alveolar spaces). The two animal models did not show the same histopathological pattern following hMPV infection. In mice, infiltration was observed on day 3 postinfection and peaked on day 5; pathological abnormalities gradually decreased thereafter (Fig. 4A). However, hMPV-infected mice continued to demonstrate greater HPS than sham-infected mice on day 21 postinfection. In cotton rats, significant cellular infiltration was only observed on days 5 (peak) and 7 postinfection (Fig. 4B). Cellular infiltration surrounding bronchioles (peribronchiolitis) of cotton rats was also more significant than in mice. Inflammatory changes in whole lungs of hMPV-infected cotton rats were similar to those described for the left lung on day 5 postinfection, and similar HPS was observed. A few infiltrating cells were found around bronchioles of sham-infected mice and cotton rats over time; this was not unexpected, since this is the interface between the nonsterile outside world and the sterile lung parenchyma and such inflammatory cells are frequently present in control animals.

Cellular infiltration in BAL samples of hMPV-infected animals. To further characterize the inflammatory response, the recruitment of inflammatory cells in BAL specimens of mice and cotton rats was monitored over time (Fig. 5). In mice, neutrophil counts increased rapidly, peaked on day 1 postinfection, and then decreased gradually until day 7. Monocyte/macrophage cell counts increased significantly from day 1 to day 3 postinfection, whereas lymphocyte counts increased on day 3 and peaked on day 5 postinfection. No changes in the amount of eosinophils were observed. In cotton rats, the neutrophils were the predominant leukocyte fraction until day 7 postinfection. Monocyte/macrophage cell counts were lower than in the mice, whereas lymphocytes slowly increased until day 7.

Pulmonary cytokine responses to hMPV infection in mice and cotton rats. In lungs of hMPV-infected mice, levels of IFN-γ, RANTES, MIP-1α, and IL-4 peaked on day 5 postinfection; such levels were significantly increased compared to those in sham-infected animals (Fig. 6). MCP-1 was detected at the highest levels on day 1 postinfection, and the mouse IL-8 homologue KC also peaked on day 1. Similarly, in lungs of hMPV-infected cotton rats, IFN-γ, RANTES, MIP-1α, and IL-2 peaked on day 5 postinfection; MCP-1 was detected at the highest levels on day 1 (Fig. 7). All cytokines levels were significantly increased compared to sham-infected animals.

DISCUSSION

We have characterized the pathogenesis of hMPV infection in two different small-animal models (BALB/c mice and cotton rats) and showed significant hMPV replication in the lower respiratory tract of both animals. After an intranasal challenge of 10^8 $TCID_{50}$, virus titers found in lung homogenates peaked on day 5 postinfection in both models (mean, 1.92×10^7 $TCID_{50}$/g in mice and 1.03×10^5 $TCID_{50}$/g in cotton rats). Of note, clinical signs of illness were only present in mice and consisted of weight loss and some breathing difficulties that peaked on days 5 to 7 postinfection. Similarly, the inflammatory cytokines and chemokines MIP-1α, IL-4 (measured in

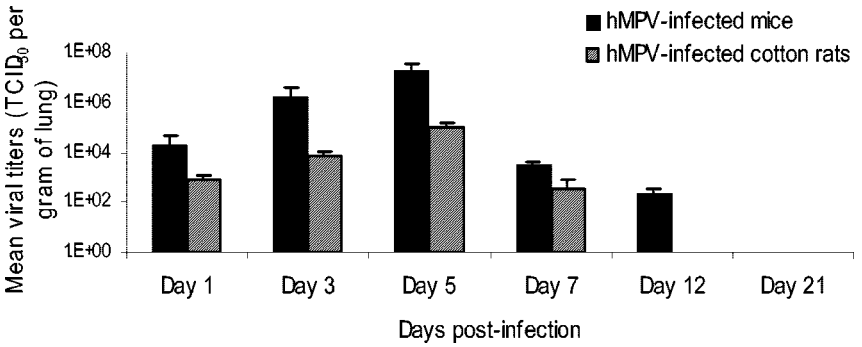

FIG. 2. Human metapneumovirus replication in lungs of BALB/c mice and cotton rats. Six mice (solid bars) and six cotton rats (hatched bars) were sacrificed on days 1, 3, 5, 7, 12, and 21 postinfection, and their lungs were removed. Lung homogenates were serially diluted and inoculated on LLC-MK2 cells for viral titration.

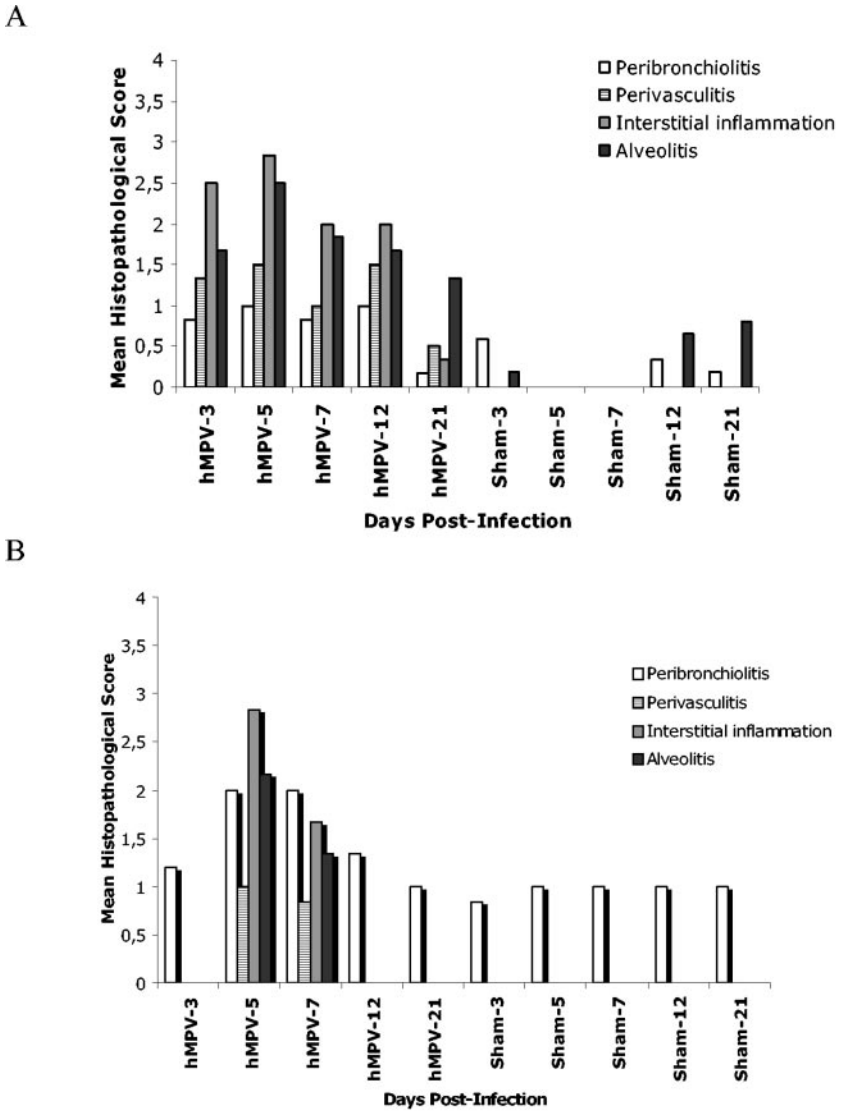

FIG. 3. Histopathological scores in hMPV- and sham-infected mice and cotton rats. The degree of lung inflammation (mean histopathologic score) was evaluated for peribronchial, perivascular, interstitial, and alveolar areas in mice (A) and cotton rats (B). The histopathological score was defined as described previously (35).

mice only), IL-2 (measured in cotton rats only), RANTES, and IFN-γ, as well as the HPS, were highest on day 5 in both models. Overall, our data suggest that BALB/c mice are more susceptible to hMPV infection than cotton rats on the basis of higher virus titers and levels of lung inflammation, combined with significant clinical signs.

HMPV is a respiratory pathogen belonging to the same subfamily (*Pneumovirinae*) as hRSV. The two paramyxoviruses have been associated with bronchiolitis and pneumonia in young children (9, 17, 23, 48). Although some primates are permissible to hMPV (26, 28, 42) and hRSV (11) infections, we selected to study BALB/c mice and cotton rats as possible experimental models for hMPV infection because those small animals are considered useful and practical models for characterizing the pathogenesis of hRSV infection and for evaluating therapeutic and prophylactic approaches (7, 11, 12, 19, 22, 24, 33, 38, 39, 41, 45, 46, 50).

Other groups have briefly reported the use of small animal exprimental models for studying hMPV infection. For instance, MacPhail et al. observed low hMPV titers in the lungs of BALB/c mice and cotton rats, following an intranasal challenge of 10^6 PFU (i.e., $10^{2.4}$ and $<10^{1.8}$ PFU/g of lung, respectively, on day 4 postinfection) (28). Furthermore, no clinical signs were observed in those animals. Hamsters and ferrets were also studied, with the highest hMPV titers (i.e., mean of $10^{4.3}$ to $10^{4.5}$ PFU/g) detected in lungs of Syrian golden hamsters on day 3 postinfection (28, 40). Of note, Skiadopoulos et al. also observed significant hMPV lung titers ($10^{4.4}$ $TCID_{50}$/g) in hamsters following an intranasal challenge of 10^6 $TCID_{50}$ (37). Similarly, no symptoms have been noted in hamsters and ferrets. However, in all the above studies, the time of peak viral replication was uncertain because no time course indicating increases or decreases in hMPV titers was reported. Recently, Alvarez et al. have reported efficient hMPV replication in

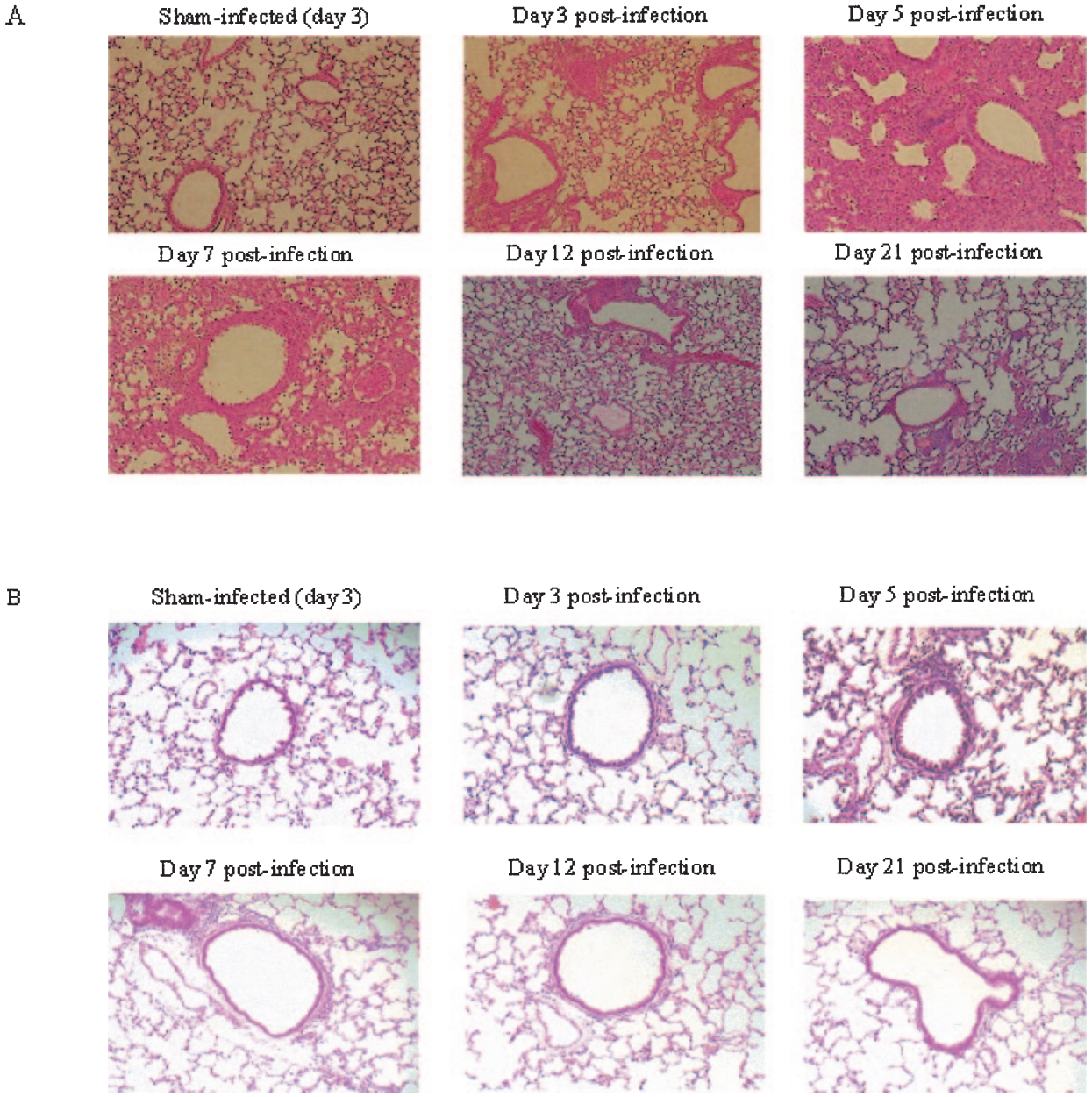

FIG. 4. Lung histopathology of hMPV- and sham-infected mice and cotton rats. (A) Six mice per group were sacrificed at different times postinfection, and their lungs were removed and fixed with 10% formalin. Thin sections of paraffin-embedded lung tissues were cut and stained with hematoxylin and eosin. A representative section (magnification, ×10) is shown for sham-infected mice on day 3 and hMPV-infected mice on days 3, 5, 7, 12, and 21 postinfection. Lung histopathology of sham-infected mice at different time points was similar to that shown on day 3. (B) Representative sections (magnification, ×20) of cotton rat lungs are shown for sham-infected rats on day 3 and for the same days postinfection as the mice.

lungs of BALB/c mice associated with transient weight loss (1). In contrast to our results, Alvarez et al. found biphasic growth kinetics for hMPV (peak titers on days 7 and 14) with prolonged viral replication in the lungs up to day 60 postinfection. A potential confounding factor between the two studies might be the selection of the viral strain, which could affect virulence and pathogenesis. Of note, we used a low-passage clinical hMPV strain belonging to the A genotype (in contrast to the extensively cell-passaged group B virus of Alvarez et al.).

It has been shown that a high viral inoculum is required to observe significant viral replication and clinical changes in lungs of hRSV-infected mice (22). Furthermore, it was shown that there is a clear dose-dependent effect of the inoculum on the severity of hRSV infection in mice (22), and our data suggest that a similar dose-dependent relationship can also be true for hMPV. We used an inoculum that was 2 logs higher (i.e., 10^8 $TCID_{50}$) than the one reported by Skiadopoulos et al. for hamsters (37). Similarly, we found a 2.5-log-higher increase in lung virus titers (i.e., 10^7 versus $10^{4.4}$ $TCID_{50}$/g) that could explain the clinical signs observed in our mouse model.

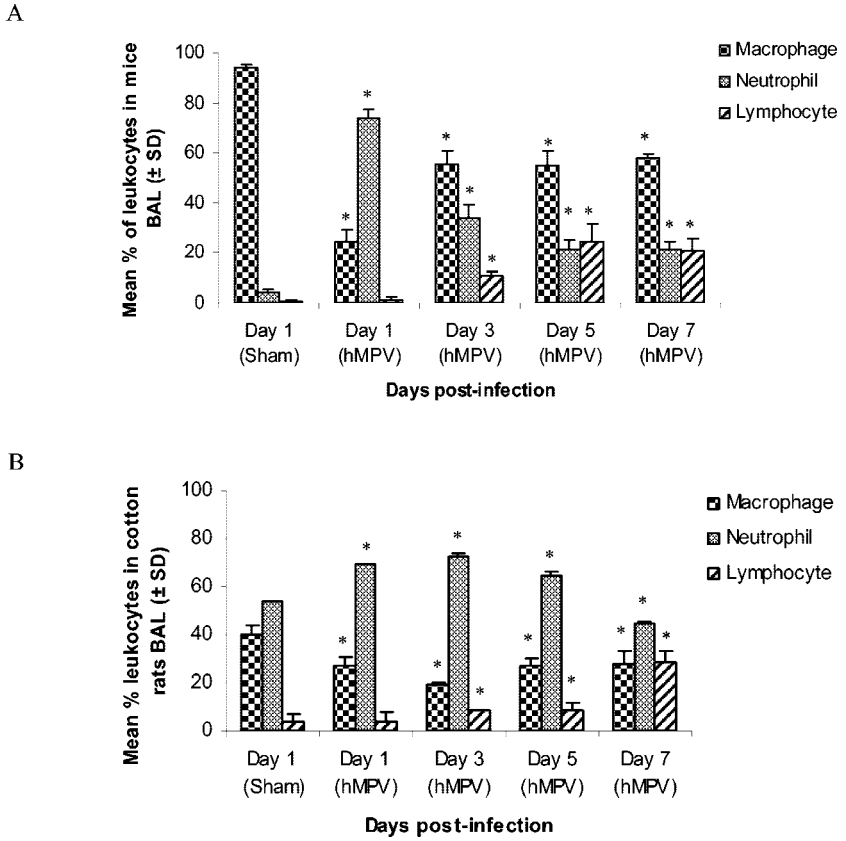

FIG. 5. Recruitment of inflammatory cells in BAL of hMPV- and sham-infected mice and cotton rats. (A) Six mice were sacrificed at different times postinfection (days 1, 3, 5, and 7), and BAL fluids were collected. Total leukocyte populations were determined using an hemacytometer, and then 2.5×10^5 cells were spotted on a slide with a cytospin. Specific cell populations were distinguished with a hematoxylin-eosin stain. Leukocyte counts were similar on all days in sham-infected mice. No changes in the amount of eosinophils were observed. (B) Six cotton rats were sacrificed at different times postinfection (days 1, 3, 5, and 7), and BAL fluids were collected. A total of 10^4 cells were used to perform a fluorescence-activated cell sorter assay to distinguish specific cell populations. *, statistically significant differences ($P < 0.05$) were observed between hMPV-infected and sham-infected groups, based on the Mann-Whitney rank sum test. SD, standard deviation.

Many similarities can be found between hMPV and hRSV replication in BALB/c mice. Following an intranasal challenge, hRSV lung titers peak on day 4 postinfection with no viruses usually recovered beyond day 7 (22, 29). On the other hand, hMPV titers peaked on day 5 in our model and viruses could still be recovered on day 12 but not by day 21 (Fig. 2). Weight loss associated with hMPV infection in mice was maximal on day 7 postinfection, 2 days after maximal viral replication, which is also similar to hRSV-induced disease in the same animal (13, 25, 46). Overall, the kinetics of hMPV replication in our mouse model are similar to those induced by hRSV and are somewhat different than those reported by Alvarez et al., i.e., a biphasic peak of replication with prolonged excretion (1). Viral replication in the lungs of cotton rats was also higher in our study (i.e., 10^5 $TCID_{50}$/g following a challenge of 10^8 $TCID_{50}$), compared to a previous research that found no detectable virus in the lungs following a challenge of 10^6 PFU (28). Of note, the latter group determined the titers for the virus by immunostaining, whereas we quantified viral growth by determination of $TCID_{50}$. Similar to hRSV infection in cotton rats (34), no clinical manifestations were noted following hMPV replication in our study.

Histopathological changes observed at the time of maximal viral replication in hMPV-infected mice mainly consisted of an interstitial inflammation characterized by an increased thickness of the alveolar walls. Cellular infiltration in the BAL of mice initially consisted of neutrophils followed by increased amounts of macrophages and lymphocytes. Of note, peribronchiolitis was more prominent in hMPV-infected cotton rats, and cellular infiltration in BAL was also somewhat different. These histopathological changes could support clinical findings indicating that hMPV may trigger exacerbations of asthma in humans (23, 31). The more severe disease observed with mice than with cotton rats may be due to the larger amounts of inflammatory cells within the alveolar spaces of mice that persisted for a longer period of time (from days 3 to 21 postinfection) (Fig. 3 and 4A). Interestingly, a significant inflammatory response was still present in lungs of mice sacrificed on day 21, although no infectious viruses could be recovered at that time. Such persistent inflammatory changes have been described for up to 154 days in mice following hRSV infection and consisted of the presence of inflammatory infiltrates located around vessels and airways (22). In contrast, we found a predominant alveolitis on day 21 postinfection; experiments

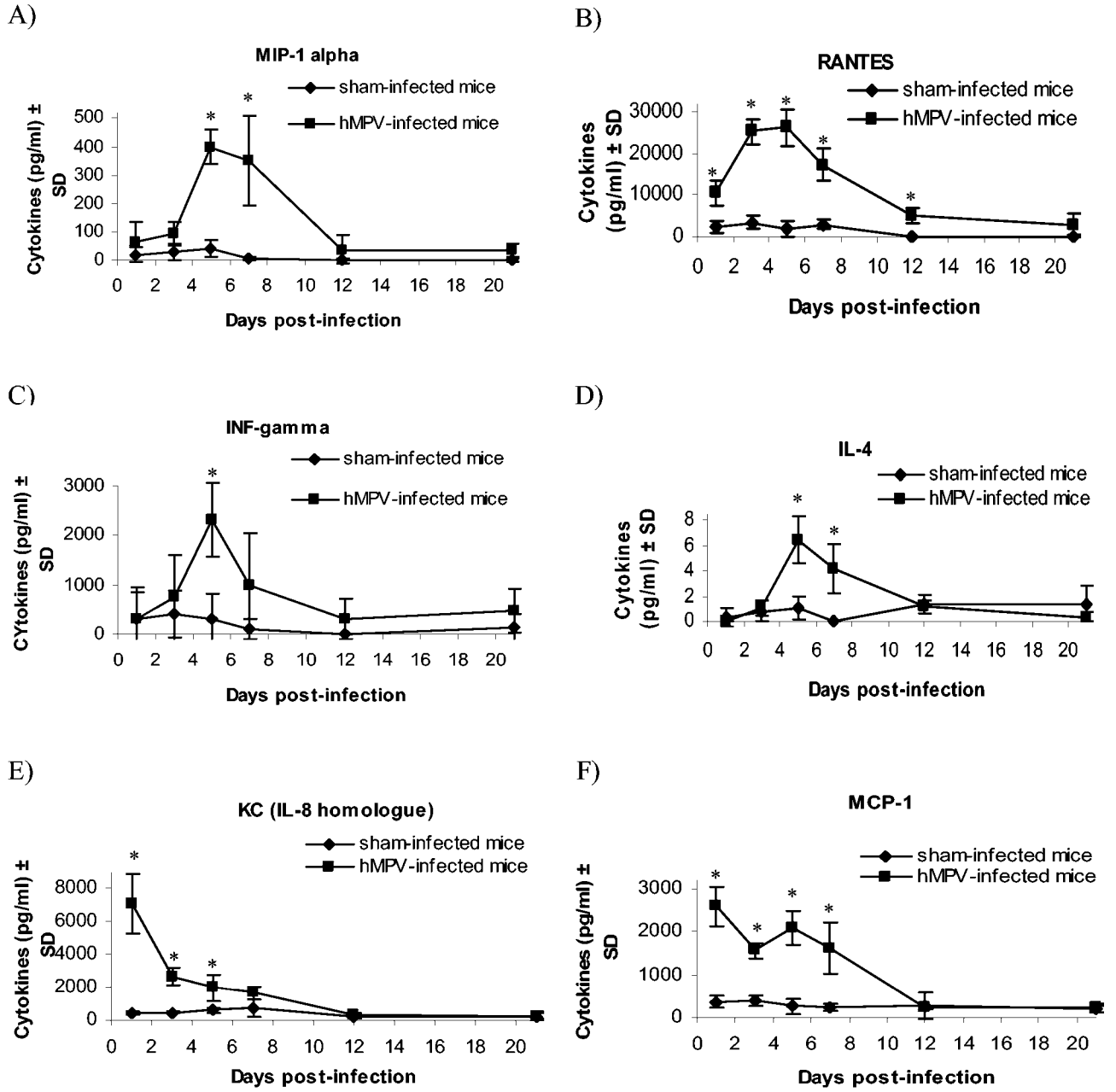

FIG. 6. Cytokine/chemokine levels in lung homogenates of hMPV- and sham-infected mice. Six mice from both hMPV- and sham-infected groups were sacrificed on days 1, 3, 5, 7, 12, and 21 postinfection, and 50 μl of their lung homogenates was used to quantify MIP-1α (A), RANTES (B), IFN-γ (C), IL-4 (D), KC (E), and MCP-1 (F) by enzyme-linked immunosorbent assay. *, statistically significant differences ($P < 0.05$) were observed between hMPV- and sham-infected groups, based on Student's *t* test when data were normally distributed and on the Mann-Whitney rank sum test when data were not normally distributed. SD, standard deviation.

are currently in progress to determine the duration of this inflammatory response. It is interesting that such chronic inflammatory changes of the airways with intra-alveolar foamy and hemosiderin-laden macrophages have been reported in humans with severe hMPV infections (47). Recent evidences have indicated that both hRSV (36) and hMPV (1) RNA can be detected for ≥100 days postinfection in lungs of BALB/c mice despite the presence of neutralizing antibodies, suggesting a state of viral latency or persistence.

In mice, high concentrations of proinflammatory cytokines are found in BAL samples following hRSV infection. KC, the mouse IL-8 homologue, is a potent chemoattractant of neutrophils that are involved in the early inflammatory response (2, 4, 22). We observed a similar pattern following hMPV infection in mice, i.e., KC levels were highest in lung homogenates on day 1 postinfection. Such high concentrations of this chemokine in hMPV-infected lung homogenates correlated with high levels of neutrophils in BAL samples. Interestingly,

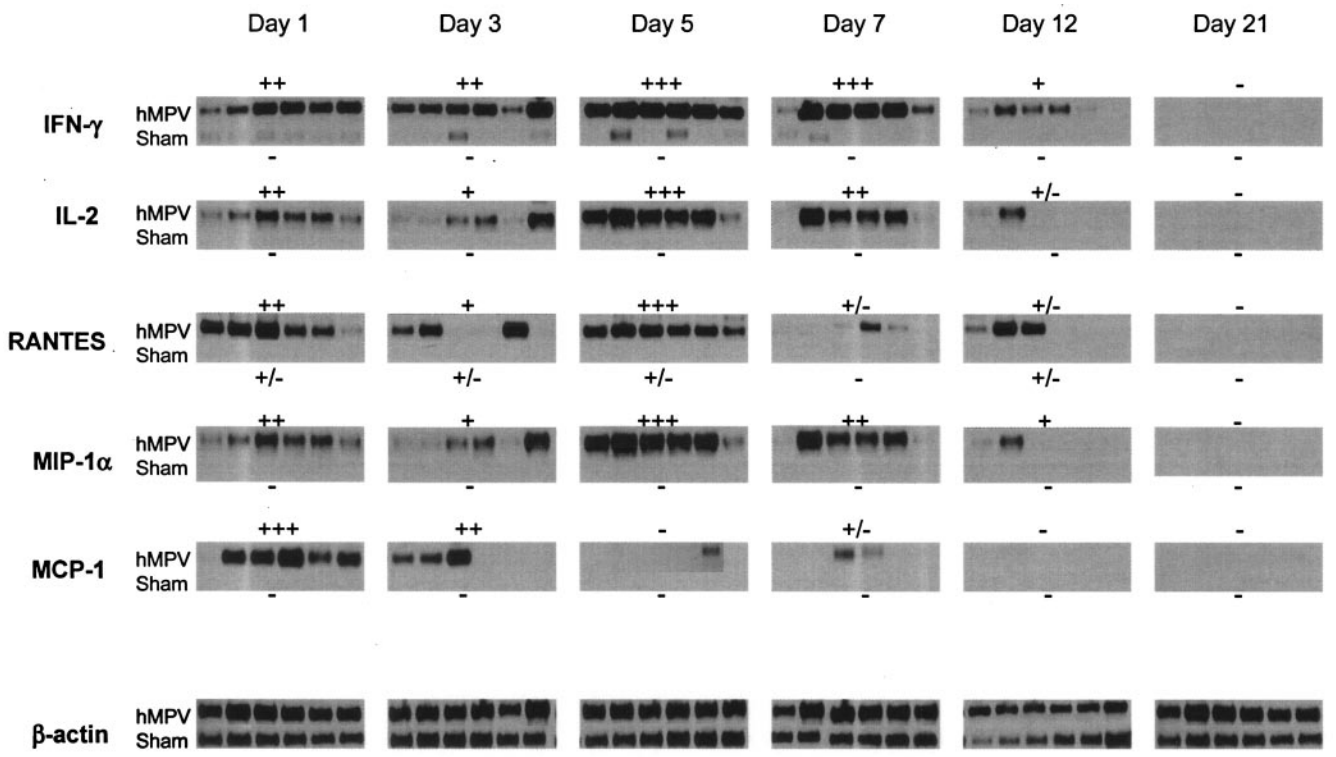

FIG. 7. Cytokine/chemokine mRNA expression in lungs homogenates of hMPV- and sham-infected cotton rats. Cotton rat lung cytokines mRNA were quantified and normalized with β-actin. A reverse transcription reaction using oligo(dT) primers was done with total lung RNA, and 50 pg of cDNA constructs was loaded to run the PCR. Detection of lung cytokines by Southern blotting was semiquantitatively measured (+ to +++). Plus signs indicate the mean degree of intensity for six cotton rats for the bands targeting the specific cytokine.

IL-8 has also been detected in upper respiratory tract secretions of hMPV-infected patients, although levels were significantly lower than those found in hRSV-infected individuals (27).

The chemokine MCP-1 is a potent chemoattractant for monocytes/macrophages and lymphocytes and has also been shown to be involved in the regulation of Th1/Th2 lymphocyte differentiation by increasing IL-4 production to enhance the Th2 response. In both mice and cotton rat models, MCP-1 was highly expressed on day 1 until day 3 to 5 postinfection, correlating with increased IL-4 production on day 5. Our results are in line with those of Barends et al., who showed that some paramyxoviruses (hRSV and pneumonia virus of mice) but not orthomyxoviruses such as influenza A are able to enhance the Th2 immune response in BALB/c mice (3).

The chemokines RANTES and MIP-1α as well as the (Th1) cytokine IFN-γ have been shown to be associated with the severity of hRSV disease (7, 13, 18, 19, 30, 46). We found that levels of those three chemokines/cytokines were significantly increased in lungs of hMPV-infected mice and cotton rats and that they all peaked at the time of maximal viral replication. Compared to findings with the mouse model of hRSV infection, we did not notice high levels of MIP-1α on day 1 postinfection; importantly, peak levels of IFN-γ were lower in hMPV-infected mice (22). This latter observation is also in line with the lower severity of hMPV infections in children (compared to that of hRSV) observed in many studies (9, 44, 48).

In conclusion, we performed a thorough investigation of hMPV infection and the resulting inflammatory/immune responses in convenient experimental animal models. We demonstrated that both BALB/c mice and cotton rats support hMPV replication in their lower respiratory tract and that such viral replication is associated with significant histopathological changes in both models, although clinical signs of illness were only observed with mice. As reported in mouse models of hRSV infection, a chronic inflammatory phase seems to occur after viral clearance (i.e., beyond day 21) that is mainly characterized by the involvement of alveolar septa and space with inflammatory cells. Whether such inflammatory change is associated with impaired pulmonary functions needs to be studied. The high levels of many proinflammatory cytokines in the lungs of hMPV-infected mice and cotton rats may indicate that an exaggerated immune response plays a significant role in the clinical manifestations of hMPV infection, similar to what has been reported for hRSV. Such experimental models will greatly contribute to further evaluation of different therapeutic agents and vaccine candidates against this important viral pathogen.

REFERENCES

1. **Alvarez, R., K. S. Harrod, W. J. Shieh, S. Zaki, and R. A. Tripp.** 2004. Human metapneumovirus persists in BALB/c mice despite the presence of neutralizing antibodies. J. Virol. **78:**14003–14011.
2. **Arnold, R., F. Werner, B. Humbert, H. Werchau, and W. Konig.** 1994. Effect of respiratory syncytial virus-antibody complexes on cytokine (IL-8, IL-6, TNF-alpha) release and respiratory burst in human granulocytes. Immunology **82:**184–191.
3. **Barends, M., L. G. de Rond, J. Dormans, M. van Oosten, A. Boelen, H. J. Neijens, A. D. Osterhaus, and T. G. Kimman.** 2004. Respiratory syncytial

virus, pneumonia virus of mice, and influenza A virus differently affect respiratory allergy in mice. Clin. Exp. Allergy **34:**488–496.
4. **Becker, S., J. Quay, and J. Soukup.** 1991. Cytokine (tumor necrosis factor, IL-6, and IL-8) production by respiratory syncytial virus-infected human alveolar macrophages. J. Immunol. **147:**4307–4312.
5. **Biacchesi, S., M. H. Skiadopoulos, G. Boivin, C. T. Hanson, B. R. Murphy, P. L. Collins, and U. J. Buchholz.** 2003. Genetic diversity between human metapneumovirus subgroups. Virology **315:**1–9.
6. **Blanco, J. C., L. Pletneva, M. Boukhvalova, J. Y. Richardson, K. A. Harris, and G. A. Prince.** 2004. The cotton rat: an underutilized animal model for human infectious diseases can now be exploited using specific reagents to cytokines, chemokines, and interferons. J. Interferon Cytokine Res. **24:**21–28.
7. **Blanco, J. C., J. Y. Richardson, M. E. Darnell, A. Rowzee, L. Pletneva, D. D. Porter, and G. A. Prince.** 2002. Cytokine and chemokine gene expression after primary and secondary respiratory syncytial virus infection in cotton rats. J. Infect. Dis. **185:**1780–1785.
8. **Boivin, G., Y. Abed, G. Pelletier, L. Ruel, D. Moisan, S. Cote, T. C. Peret, D. D. Erdman, and L. J. Anderson.** 2002. Virological features and clinical manifestations associated with human metapneumovirus: a new paramyxovirus responsible for acute respiratory-tract infections in all age groups. J. Infect. Dis. **186:**1330–1334.
9. **Boivin, G., G. De Serres, S. Cote, R. Gilca, Y. Abed, L. Rochette, M. G. Bergeron, and P. Dery.** 2003. Human metapneumovirus infections in hospitalized children. Emerg. Infect. Dis. **9:**634–640.
10. **Boivin, G., I. Mackay, T. P. Sloots, S. Madhi, F. Freymuth, D. Wolf, Y. Shemer-Avni, H. Ludewick, G. C. Gray, and E. LeBlanc.** 2004. Global genetic diversity of human metapneumovirus fusion gene. Emerg. Infect. Dis. **10:**1154–1157.
11. **Byrd, L. G., and G. A. Prince.** 1997. Animal models of respiratory syncytial virus infection. Clin. Infect. Dis. **25:**1363–1368.
12. **Curtis, S. J., M. G. Ottolini, D. D. Porter, and G. A. Prince.** 2002. Age-dependent replication of respiratory syncytial virus in the cotton rat. Exp. Biol. Med. (Maywood). **227:**799–802.
13. **Durbin, J. E., T. R. Johnson, R. K. Durbin, S. E. Mertz, R. A. Morotti, R. S. Peebles, and B. S. Graham.** 2002. The role of IFN in respiratory syncytial virus pathogenesis. J. Immunol. **168:**2944–2952.
14. **Ebihara, T., R. Endo, H. Kikuta, N. Ishiguro, M. Yoshioka, X. Ma, and K. Kobayashi.** 2003. Seroprevalence of human metapneumovirus in Japan. J. Med. Virol. **70:**281–283.
15. **Esper, F., D. Boucher, C. Weibel, R. A. Martinello, and J. S. Kahn.** 2003. Human metapneumovirus infection in the United States: clinical manifestations associated with a newly emerging respiratory infection in children. Pediatrics **111:**1407–1410.
16. **Falsey, A. R., D. Erdman, L. J. Anderson, and E. E. Walsh.** 2003. Human metapneumovirus infections in young and elderly adults. J. Infect. Dis. **187:** 785–790.
17. **Freymouth, F., A. Vabret, L. Legrand, N. Eterradossi, F. Lafay-Delaire, J. Brouard, and B. Guillois.** 2003. Presence of the new human metapneumovirus in French children with bronchiolitis. Pediatr. Infect. Dis. J. **22:**92–94.
18. **Garofalo, R. P., J. Patti, K. A. Hintz, V. Hill, P. L. Ogra, and R. C. Welliver.** 2001. Macrophage inflammatory protein-1alpha (not T helper type 2 cytokines) is associated with severe forms of respiratory syncytial virus bronchiolitis. J. Infect. Dis. **184:**393–399.
19. **Haeberle, H. A., W. A. Kuziel, H. J. Dieterich, A. Casola, Z. Gatalica, and R. P. Garofalo.** 2001. Inducible expression of inflammatory chemokines in respiratory syncytial virus-infected mice: role of MIP-1α in lung pathology. J. Virol. **75:**878–890.
20. **Hamelin, M. E., Y. Abed, and G. Boivin.** 2004. Human metapneumovirus: a new player among respiratory viruses. Clin. Infect. Dis. **38:**983–990.
21. **Ishiguro, N., T. Ebihara, R. Endo, X. Ma, H. Kikuta, H. Ishiko, and K. Kobayashi.** 2004. High genetic diversity of the attachment (G) protein of human metapneumovirus. J. Clin. Microbiol. **42:**3406–3414.
22. **Jafri, H. S., S. Chavez-Bueno, A. Mejias, A. M. Gomez, A. M. Rios, S. S. Nassi, M. Yusuf, P. Kapur, R. D. Hardy, J. Hatfield, B. B. Rogers, K. Krisher, and O. Ramilo.** 2004. Respiratory syncytial virus induces pneumonia, cytokine response, airway obstruction, and chronic inflammatory infiltrates associated with long-term airway hyperresponsiveness in mice. J. Infect. Dis. **189:**1856–1865.
23. **Jartti, T., B. van den Hoogen, R. P. Garofalo, A. D. Osterhaus, and O. Ruuskanen.** 2002. Metapneumovirus and acute wheezing in children. Lancet **360:**1393–1394.
24. **Johnson, S. A., M. G. Ottolini, M. E. Darnell, D. D. Porter, and G. A. Prince.** 1996. Unilateral nasal infection of cotton rats with respiratory syncytial virus allows assessment of local and systemic immunity. J. Gen. Virol. **77:**101–108.
25. **Johnson, T. R., M. N. Teng, P. L. Collins, and B. S. Graham.** 2004. Respiratory syncytial virus (RSV) G glycoprotein is not necessary for vaccine-enhanced disease induced by immunization with formalin-inactivated RSV. J. Virol. **78:**6024–6032.
26. **Kuiken, T., B. G. van den Hoogen, D. A. van Riel, J. D. Laman, G. van Amerongen, L. Sprong, R. A. Fouchier, and A. D. Osterhaus.** 2004. Experimental human metapneumovirus infection of cynomolgus macaques (Macaca fascicularis) results in virus replication in ciliated epithelial cells and pneumocytes with associated lesions throughout the respiratory tract. Am. J. Pathol. **164:**1893–1900.
27. **Laham, F. R., V. Israele, J. M. Casellas, A. M. Garcia, C. M. Lac Prugent, S. J. Hoffman, D. Hauer, B. Thumar, M. I. Name, A. Pascual, N. Taratutto, M. T. Ishida, M. Balduzzi, M. Maccarone, S. Jackli, R. Passarino, R. A. Gaivironsky, R. A. Karron, N. R. Polack, and F. P. Polack.** 2004. Differential production of inflammatory cytokines in primary infection with human metapneumovirus and with other common respiratory viruses of infancy. J. Infect. Dis. **189:**2047–2056.
28. **MacPhail, M., J. H. Schickli, R. S. Tang, J. Kaur, C. Robinson, R. A. Fouchier, A. D. Osterhaus, R. R. Spaete, and A. A. Haller.** 2004. Identification of small-animal and primate models for evaluation of vaccine candidates for human metapneumovirus (hMPV) and implications for hMPV vaccine design. J. Gen. Virol. **85:**1655–1663.
29. **Mejias, A., S. Chavez-Bueno, A. M. Rios, J. Saavedra-Lozano, M. Fonseca Aten, J. Hatfield, P. Kapur, A. M. Gomez, H. S. Jafri, and O. Ramilo.** 2004. Anti-respiratory syncytial virus (RSV) neutralizing antibody decreases lung inflammation, airway obstruction, and airway hyperresponsiveness in a murine RSV model. Antimicrob. Agents Chemother. **48:**1811–1822.
30. **Olszewska-Pazdrak, B., A. Casola, T. Saito, R. Alam, S. E. Crowe, F. Mei, P. L. Ogra, and R. P. Garofalo.** 1998. Cell-specific expression of RANTES, MCP-1, and MIP-1α by lower airway epithelial cells and eosinophils infected with respiratory syncytial virus. J. Virol. **72:**4756–4764.
31. **Peiris, J. S., W. H. Tang, K. H. Chan, P. L. Khong, Y. Guan, Y. L. Lau, and S. S. Chiu.** 2003. Children with respiratory disease associated with metapneumovirus in Hong Kong. Emerg. Infect. Dis. **9:**628–633.
32. **Peret, T. C., G. Boivin, Y. Li, M. Couillard, C. Humphrey, A. D. Osterhaus, D. D. Erdman, and L. J. Anderson.** 2002. Characterization of human metapneumoviruses isolated from patients in North America. J. Infect. Dis. **185:** 1660–1663.
33. **Prince, G. A., C. Capiau, M. Deschamps, L. Fabry, N. Garcon, D. Gheysen, J. P. Prieels, G. Thiry, O. Van Opstal, and D. D. Porter.** 2000. Efficacy and safety studies of a recombinant chimeric respiratory syncytial virus FG glycoprotein vaccine in cotton rats. J. Virol. **74:**10287–10292.
34. **Prince, G. A., A. B. Jenson, R. L. Horswood, E. Camargo, and R. M. Chanock.** 1978. The pathogenesis of respiratory syncytial virus infection in cotton rats. Am. J. Pathol. **93:**771–791.
35. **Prince, G. A., J. P. Prieels, M. Slaoui, and D. D. Porter.** 1999. Pulmonary lesions in primary respiratory syncytial virus infection, reinfection, and vaccine-enhanced disease in the cotton rat (Sigmodon hispidus). Lab. Investig. **79:**1385–1392.
36. **Schwarze, J., D. R. O'Donnell, A. Rohwedder, and P. J. Openshaw.** 2004. Latency and persistence of respiratory syncytial virus despite T cell immunity. Am. J. Respir. Crit. Care Med. **169:**801–805.
37. **Skiadopoulos, M. H., S. Biacchesi, U. J. Buchholz, J. M. Riggs, S. R. Surman, E. Amaro-Carambot, J. M. McAuliffe, W. R. Elkins, M. St. Claire, P. L. Collins, and B. R. Murphy.** 2004. The two major human metapneumovirus genetic lineages are highly related antigenically, and the fusion (F) protein is a major contributor to this antigenic relatedness. J. Virol. **78:**6927–6937.
38. **Steward, M. W.** 2001. The development of a mimotope-based synthetic peptide vaccine against respiratory syncytial virus. Biologicals **29:**215–219.
39. **Sudo, K., W. Watanabe, S. Mori, K. Konno, S. Shigeta, and T. Yokota.** 1999. Mouse model of respiratory syncytial virus infection to evaluate antiviral activity in vivo. Antivir. Chem. Chemother. **10:**135–139.
40. **Tang, R. S., J. H. Schickli, M. MacPhail, F. Fernandes, L. Bicha, J. Spaete, R. A. Fouchier, A. D. Osterhaus, R. Spaete, and A. A. Haller.** 2003. Effects of human metapneumovirus and respiratory syncytial virus antigen insertion in two 3′ proximal genome positions of bovine/human parainfluenza virus type 3 on virus replication and immunogenicity. J. Virol. **77:**10819–10828.
41. **Trudel, M., F. Nadon, C. Seguin, and H. Binz.** 1991. Protection of BALB/c mice from respiratory syncytial virus infection by immunization with a synthetic peptide derived from the G glycoprotein. Virology **185:**749–757.
42. **van den Hoogen, B. G., J. C. de Jong, J. Groen, T. Kuiken, R. de Groot, R. A. Fouchier, and A. D. Osterhaus.** 2001. A newly discovered human pneumovirus isolated from young children with respiratory tract disease. Nat. Med. **7:**719–724.
43. **van den Hoogen, B. G., S. Herfst, L. Sprong, P. A. Cane, E. Forleo-Neto, R. L. de Swart, A. D. Osterhaus, and R. A. Fouchier.** 2004. Antigenic and genetic variability of human metapneumoviruses. Emerg. Infect. Dis. **10:**658–666.
44. **van den Hoogen, B. G., G. J. Van Doornum, J. C. Fockens, J. J. Cornelissen, W. E. Beyer, R. de Groot, A. D. Osterhaus, and R. A. Fouchier.** 2003. Prevalence and clinical symptoms of human metapneumovirus infection in hospitalized patients. J. Infect. Dis. **188:**1571–1577.
45. **van Schaik, S. M., G. Enhorning, I. Vargas, and R. C. Welliver.** 1998. Respiratory syncytial virus affects pulmonary function in BALB/c mice. J. Infect. Dis. **177:**269–276.
46. **van Schaik, S. M., N. Obot, G. Enhorning, K. Hintz, K. Gross, G. E. Hancock, A. M. Stack, and R. C. Welliver.** 2000. Role of interferon gamma in the pathogenesis of primary respiratory syncytial virus infection in BALB/c mice. J. Med. Virol. **62:**257–266.
47. **Vargas, S. O., H. P. Kozakewich, A. R. Perez-Atayde, and A. J. McAdam.** 2004. Pathology of human metapneumovirus infection: insights into the

pathogenesis of a newly identified respiratory virus. Pediatr. Dev. Pathol. **7:**478–486.

48. **Viazov, S., F. Ratjen, R. Scheidhauer, M. Fiedler, and M. Roggendorf.** 2003. High prevalence of human metapneumovirus infection in young children and genetic heterogeneity of the viral isolates. J. Clin. Microbiol. **41:**3043–3045.
49. **Wolf, D. G., Z. Zakay-Rones, A. Fadeela, D. Greenberg, and R. Dagan.** 2003. High seroprevalence of human metapneumovirus among young children in Israel. J. Infect. Dis. **188:**1865–1867.
50. **Zhang, Y., Y. Wang, X. Gilmore, K. Xu, P. R. Wyde, and I. N. Mbawuike.** 2002. An aged mouse model for RSV infection and diminished CD8(+) CTL responses. Exp. Biol. Med. **227:**133–140.